A MEMS-Based Monolithic Electrostatic Microactuator for Ultra-Low Magnetic Disk Head Fly Height Control

Fang Chen, Huikai Xie, and Gary K. Fedder

Abstract—A novel MEMS-based electrostatic actuator design is proposed for recording head fly height control below 10 nm. Different from prior work on MEMS-based electrostatic microactuators designed for magnetic hard disk drives (HDD), the proposed microactuator is fabricated monolithically with a conventional head/slider design. The actuator is micromachined into the same side as the head element on a slider with a modified CMOS-MEMS process. It has an extremely small size, light weight and a very simple structure. The head is suspended and actuated up and down by the actuator during recording process to maintain a constant fly height. A desired range and precision of actuation is achieved under control voltages of less than 30 V. A mechanical resonant frequency of over 100 kHz is obtained.

Index Terms—Fly height, MEMS electrostatic actuator, microfabrication, slider.

I. INTRODUCTION

IN THE magnetic HDD, the recording head is attached to the end tip of an air-bearing slider. The rapid spinning of the disk creates a thin air cushion between the air-bearing surface (ABS) and the disk surface. This aerodynamic property allows the slider to fly above the surface and make a slight angle with the disk level. The recording head, which is located at the trailing edge of the slider, defines the smallest distance toward the surface—the fly height.

The fly height of current state-of-the-art sliders for advanced magnetoresistance (MR) head is about 12.5 nm and will have to reduce to below 10 nm to achieve an areal density of 100 Gbits/in^2. The sub-10 nm fly height will eventually require an actuation mechanism with sub-nanometer precision in addition to a self-acting air-bearing in fly height control. Factors that can change the fly height during recording are disturbances of velocity, mechanical shock, air pressure, temperature and dust, disk roughness and asperities, as well as wear of the ABS due to contact with the disk surface. There is also a fly height change problem associated with the head traversing the disk in
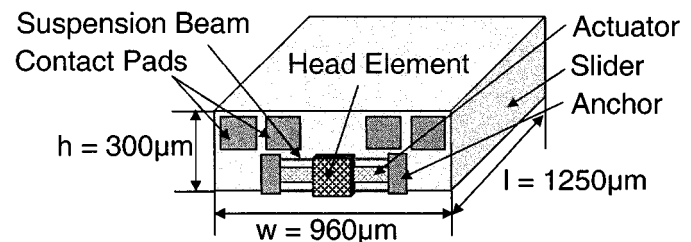
Fig. 1. Concept for a monolithic MEMS-based slider/actuator/head-element structure. The dimension is typical for a pico-slider.

and out [1]. The air-bearing method alone will not be sufficient to maintain sub-10 nm fly height specification.

MEMS based microactuators have been proposed recently for HDD servo control. MEMS based *z*-height actuator is a possible solution in the future for all the problems mentioned above. In this paper, such a MEMS-based electrostatic microactuator for sub-10 nm fly height application is proposed. Different from prior work on MEMS-based electrostatic microactuator designed for HDD [2]–[8], the proposed microactuator is to be fabricated monolithically with a conventional head/slider design. This microactuation mechanism will serve as a secondary control to the air-bearing method to provide further precision and stability.

II. DESIGN AND FABRICATION

A. Basic Concept

The basic concept for this design is to fabricate a monolithic slider/actuator/head-element structure from a single wafer. The actuator structure resides on the trailing-edge side of the slider with the head. The head element is completely released from the substrate and suspended by spring beams. The concept is illustrated in Fig. 1. The actuation is provided by an electrostatic parallel-plate actuator and the head is connected to the substrate by flexures to provide rigidity. The slider shown is a typical pico-slider that is 1250 μm in length, 950 μm in width and 300 μm in thickness. In this design, we assume that the head element can be fabricated into an 80 μm by 80 μm area. The electrical bonding pads for the heads are placed outside on the substrate and the connection between contacts and pads are made through special structure layout via the microactuator beams and deposited metal layers. The details of the wiring will be discussed in Section II-C.

TABLE I
MICROACTUATOR SPECIFICATIONS

Structure size	~ 450 μm x 100 μm
Load mass	~ 1μg
Applied voltage	< 30V
Mechanical resonance frequency	> 100 kHz
z-direction stroke	± 5 nm
Shock resistance	> 200 G
Control resolution	< 0.1 nm

TABLE II
MEMS ACTUATOR SPECIFICATIONS BY DESIGN

Length of fingers	100 μm
Width of fingers	18 μm
Effective depth of parallel plate electrodes	9 μm
Gap between electrodes	1.8 μm
Length of the beam	105 μm
Width of the beam	3.5 μm
Depth of the beam	29 μm
Gap between plate and beam	8 μm

B. Requirements and Specifications

The following factors are considered before choosing a fabrication process. First of all, low cost is probably the most important. The fabrication process should be simple, cost effective and have few additional steps. Secondly, it must facilitate slider/actuator/head integration. All fabrication processes are to be executed on one wafer. Gluing a head to the actuator or other ways of mechanically attaching a separately machined actuator and head element is not very practical when good alignment with nanometer precision must be guaranteed. Thirdly, the fabrication process must be highly consistent with the conventional head fabrication process. A list of specifications for the microactuator is given in Table I.

C. Microactuator Design

To meet the specifications discussed in the previous section, the parameters shown in the Table II are chosen for the parallel-plate microactuator and beam structure.

Fig. 2(a) is the top view of the microactuator layout. The head is suspended by four symmetrical high aspect ratio flexure beams on both sides. The actuation for the head in the $\pm z$ direction is provided by two sets of electrostatic actuators including rotor and stator fingers. The gaps between the fingers are very small in order to generate sufficient electrostatic force. However, the gaps between the flexure beam and the actuator fingers are wide in order to reduce undesired electrostatic forces. The whole structure is rigid and compact. The head element is fabricated on top of the square structure in the middle. Four metal wires for both the magnetic reader and writer are shown in Fig. 2(a) as the thin dark lines along the flexure beams providing connections between the head contacts and the bonding pads. Only a small fraction of the bonding pads is shown in Fig. 2(a). The actual size is about 200 μm by 200 μm. The wire resistance is calculated to be less than 0.25Ω.
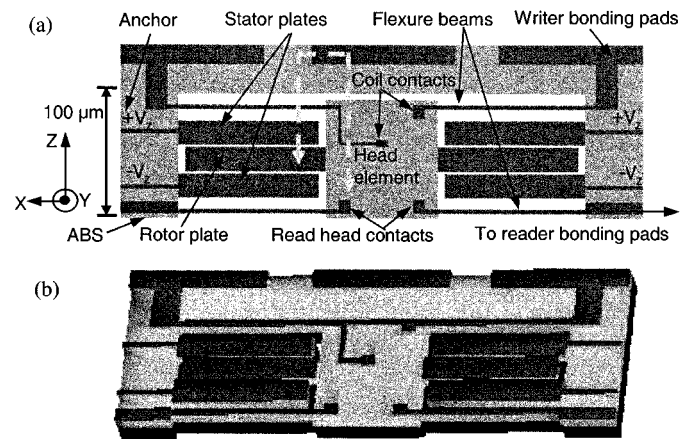

Fig. 2. (a) Layout (top view) of the microactuator structure. The dimension is about 450 μm by 120 μm. Dotted line is the cross-section in Fig. 3. (b) Solid model for finite-element analysis.
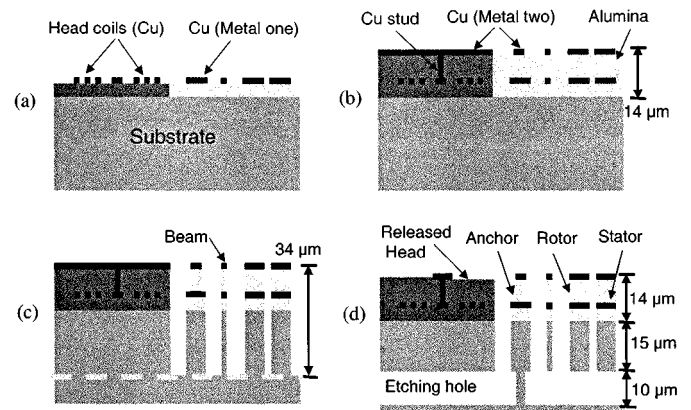

Fig. 3. Head/actuator fabrication flow (cross-section view): (a) Head coil and first metal for electrodes. (b) Complete head fabrication and pattern the second metal for electrodes. (c) DRIE to define microactuator structure. (d) Sidewall DRIE etch to release the actuator and head.

D. Fabrication Procedures

In conventional head and slider fabrication, head elements are fabricated on a wafer first, then the wafer is sliced into bars, which are lapped and ion milled to form the air-bearing surface. The bars are then diced into individual sliders. To incorporate the MEMS microactuator into the slider, the employed process is highly compatible with the head fabrication process and is very similar to the CMOS-MEMS process developed at Carnegie Mellon University [9], in which the interconnect metal layers act as an etching mask to define microstructures, and a backside deep reactive-ion-etch (RIE) is used to release the microstructures.

The procedures of the proposed fabrication are as follows:

1) A 2 μm-thick copper layer for the write head coils in the head fabrication process is used as the structural layer and part of the electrodes for the microactuator (metal one) [Fig. 3(a)].
2) The conventional head fabrication process is performed up to the insulation layer lapping and followed by deposition of a 1.5 μm thick copper (metal two) [Fig. 3(b)].
3) Using metal two as the etching mask (protecting the head), an anisotropic RIE (CHF$_3$) of alumina 14 μm is

TABLE III
MEMS ACTUATOR CHARACTERISTICS

Moving parts effective mass	~1.20 µg
Spring constant k_z	500 N/m
Spring constant k_y	34362 N/m
Spring constant k_x	450470 N/m
Maximum applied voltage	30 V
Resonant frequency	102.7 kHz
Stroke	±5.3 nm
Displacement under 200G in z	4.7 nm
Displacement under 500G in y	0.15 nm
Displacement under 500G in x	0.01 nm

TABLE IV
MODAL ANALYSIS

Modes	Frequency (kHz)	Modes	Frequency (kHz)
1. z	110.95	4. θ_x	1018.29
2. y	556.11	5. θ_y	1072.72
3. θ_z	778.70	6. Stator	1120.37

Fig. 4. (a) Shield finger from head (top view). (b) Finger cross-section.

performed, followed by another anisotropic deep RIE (DRIE) of the silicon substrate 20 µm (SF$_6$ in Bosch process) to form the microactuator structure [Fig. 3(c)].

4) The wafer is sliced into slider bars and the bars are turned to the side. A lapping process then, defines the head throat height, followed by conventional ion-milling to form the rails and ABS. Next, on the ABS near the head, a silicon DRIE is used to release the head from the bottom by etching a rectangular hole about 300 µm long, 10 µm wide and is about 34 µm from the edge of the slider shown as the dotted line in Fig. 3(c). Etching is 100 µm deep so it releases the head and the actuator structure altogether. By leaving a room of 5 µm Si to take the undercut, a 15 µm-thick Si-substrate is left to support the head element [Fig. 3(d)]. At last, the slider bars are diced into individual sliders.

This actuator design achieves the goal of actuator/head integration. The actuators are micromachined at wafer level with hundreds of them made at once. Head and slider fabrications are unaffected by adding the actuator.

III. ACTUATOR ANALYSIS

The two metal layers in the actuator beams are interconnected through vias. Using the ANSOFT Maxwell 2-D field simulator, it is found that the multi-layer beams (rotor and stator) can be modeled as electrodes of a parallel-plate capacitor. Using this approximation, the microactuator's characteristics and static responses are calculated which are shown in Table III.

The large k_z and small mass also result in very high natural resonant frequency (>100 kHz) compared to a few kHz servo bandwidth of the conventional mechanical actuator for the slider suspension arm. Due to the high aspect ratio of the beam structure achieved by DRIE processing, very large spring constants in x and y directions are obtained. The rigidity in these directions is very necessary to minimize the amount of displacement due to the outside disturbance, such as mechanical shocks and airflow. The structure guarantees a sub-nanometer off-axis displacement under 200G shock. In the x and y directions, the displacement can be ignored, while in the actuation direction, as long as the fly height is greater than 5 nm, a head-disk crash will not occur (chances will be even smaller when the system is used with closed-loop control). This small displacement is also partially attributed to the light mass of the moving structure.
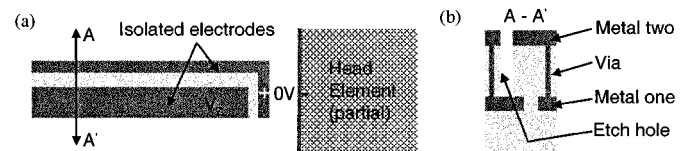
A finite element method (FEM) modal analysis was performed using MEMCAD [10] to obtain the first six resonant frequencies of the system in Table IV. The lowest resonant frequency was found at 110 kHz in the z-direction. The three torsional modes are resulted from force imbalance of the parallel-plate actuator. Since the structure is symmetric and rigid, this imbalance is small, and the corresponding resonant frequencies are much higher around 1 MHz. Fig. 2(b) is the generated 3-d model for the structure.

IV. OTHER ISSUES

The presence of the electrostatic actuator may cause ESD to the GMR sensor. Therefore shielding the finger from the head element is necessary. A possible shielding configuration of the metal layers in the fingers is shown in Fig. 4.

Dust collecting between the parallel-plates due to electrostatic attraction force will change the properties of the actuator. Dust particles having micrometer dimensions are comparable to the gap between the plates. Possible solutions are sealing off the actuator.

The fly height actuator will not work without a fly height sensor. What we need here is an *in-situ* sensor with subnanometer sensitivity. This can be done by simply using the average magnitude of the readback signal. There have been quite a few papers addressing the possibility, and as small as 0.2 nm resolution has been reported [11]. There is also research on a capacitive fly height sensor which requires deposition of films on the bottom of the slider.

V. CONCLUSION

We have proposed a MEMS-based monolithic fly height actuator to sub-10 nm application. Si-DRIE are applied to the fabrication to achieve the following critical requirements: 1) Structural high aspect ratio for the rigidity of the actuator to confine the range of motion, 2) Electrical isolation between the movable and stationary electrodes, and between actuator and silicon substrate, 3) Complete dry etch structure release for low cost, and good critical dimension control compared to wet etch, and 4) Compatibility with conventional head fabrication to facilitate actuator/head integration. The design simulation results show sub-nanometer precision in actuation, >100 kHz in bandwidth and a shock resistance of >200G.

ACKNOWLEDGMENT

REFERENCES

[1] B. Schardt *et al.*, "Flying height measurement while seeking in hard disk drives," *IEEE Trans. Magn.*, vol. 34, pp. 1765–1767, 1998.

[2] E. Narbutovskih *et al.*, "A silicon microsuspension for disk drive applications," in *Tranducers 97. Digest of Technical.*, vol. 1525, pp. 221–224.

[3] T. Imamura *et al.*, "MEMS based integrated head/actuator/slider for HDD," *IEEE/ASME Trans. Mechatronics*, vol. 3, pp. 166–174, Sept. 1998.

[4] S. Nakamura *et al.*, "Application of micromachine technologies to hard disk drives," *IEEE Trans. Magn.*, pt. 1, vol. 34, no. 2, pp. 477–479, 1998.

[5] D. Horsley *et al.*, "Microfabricated electrostatic actuators for hard disk drives," *IEEE/ASME Trans. Mechatronics*, vol. 3, pp. 175–183, Sept. 1998.

[6] T. Semba *et al.*, "Dual-stage servo controller for HDD using MEMS microactuator," *IEEE Trans. Magn.*, pt. 1, vol. 35, no. 5, pp. 2271–2273, 1999.

[7] T. Hirano *et al.*, "Micro-actuator for tera-storage," in *Technical Digest, IEEE International MEMS 99 Conference*, xxxvi+660, pp. 441–446.

[8] J. Drake and H. Jerman, "A micromachined torsional mirror for track following in magneto-optical disk drives," in *Technical Digest, Solid-State Sensor and Actuator Workshop*, Hilton Head, SC, June 4–8, 2000, pp. 10–13.

[9] H. Xie *et al.*, "Post-CMOS processing for high-aspect-ratio integrated silicon microstructures," in *Technical Digest, Solid-State Sensor and Actuator Workshop*, Hilton Head, SC, June 4–8, 2000, pp. 77–80.

[10] "User's Manual for MEMCAD 4.8," Microcosm Technologies, Inc., Cary, NC, Copyright 2000.

[11] V. J. Novotny and M.-J. Hsiao, "Sensitive magnetic readback head disk spacing measurement in recording drives," *IEEE Trans. Magn.*, vol. 34, no. 4, pp. 1762–1764, July 1998.